Turkish Journal of Physics

http://journals.tubitak.gov.tr/physics/

Research Article

Turk J Phys
(2019) 43: 372 – 382

doi:10.3906/fiz-1901-3

An investigation of structural properties and surface morphologies of electrochemically fabricated nanocrystalline Ni–Co–Cu/ITO deposits with different compositions

Umut SARAÇ[1,*], **Mevlana Celalettin BAYKUL**[2]
[1]Department of Science Education, Bartın University, Bartın, Turkey
[2]Department of Metallurgical and Materials Engineering, Faculty of Engineering, Eskişehir Osmangazi University, Eskişehir, Turkey

Received: 02.01.2019 • **Accepted/Published Online:** 10.05.2019 • **Final Version:** 02.08.2019

Abstract: In this study, nanocrystalline ternary Ni–Co–Cu/ITO deposits with different compositions were produced by using the electrochemical deposition technique from a sulfate-based bath solution with different Co ion concentrations. It was revealed that an increment in the Co ion concentration gives rise to an enhancement in the Co content but leads to a decrement in the Ni and Cu contents of the deposit structure. The Co–Cu and Ni–Cu exhibited normal codeposition behavior, while the Co–Ni showed anomalous codeposition behavior irrespective of the bath concentration. The change in the degree of the anomalous codeposition was also investigated according to the Co ion concentration. The deposits exhibited a dual face-centered cubic (fcc) phase structure comprising Cu and Ni–Co phases. The strength of the Ni–Co (111) (Cu (111)) phase increased with respect to the Cu (111) (Ni–Co (111)) phase when the Co (Cu) content in the ternary Ni–Co–Cu deposit increased. The size of the crystallites, the value of the interplanar spacing, and the crystallinity of the deposits changed depending on the deposit composition. It was also revealed that the differences in the deposit composition highly affect the average diameter and the density of the agglomerated clusters formed on the deposit surfaces.

Key words: Ternary Ni–Co–Cu deposits, anomalous codeposition, dual phase structure, crystallite size, interplanar spacing, deposit composition, surface structure

1. Introduction

The effects of operating conditions have been widely studied owing to their strong influences on the structural, magnetic, and morphological properties of the magnetic material systems grown by electrochemical deposition technique. For this reason, different Ni, Co, and Fe-based magnetic materials have been produced under different electrochemical deposition conditions [1]. Among the magnetic material systems, ternary Ni–Co–Cu deposits have interesting magnetic properties and exhibit better corrosion resistance than Co–Cu deposits [2]. Different deposition techniques have been used to produce magnetic materials. Some of them (sputtering, thermal evaporation, etc.) have complex and high-cost features; however, electrochemical deposition is a relatively cheap, ecofriendly, and simple technique [3,4]. Controlling the chemical composition of the deposit in electrochemically grown metallic alloy deposits and multilayers is a very important issue. It is well known that the ion concentration of the bath used in the fabrication process strongly affects the chemical composition

*Correspondence: usarac@bartin.edu.tr

of the deposit [4–10]. In this way, magnetic metallic materials with different compositions exhibiting different physical properties can be electrochemically obtained.

To the best of our knowledge there is no study on the compositional differences, codeposition behavior, structural properties, and surface morphologies of Ni–Co–Cu/ITO deposits electrochemically produced from sulfate-based baths with different Co ion concentrations. Therefore, an attempt was carried out to obtain ternary Ni–Co–Cu/ITO deposits with different compositions and investigate the changes in their structural properties and surface morphologies according to the deposit composition. Based on the findings obtained in this study, it was understood that not only structural properties but also surface morphologies of the resultant deposits are considerably affected by changing the deposit composition, which can be modified by controlling the Co ion concentration of the bath solution.

2. Experimental details

In the present study, ternary Ni–Co–Cu deposits were fabricated using the electrochemical deposition technique. The electrochemical fabrication processes were performed by a potentiostat/galvanostat (VersaSTAT 3) with a conventional three-electrode cell composed of reference, working, and counter electrodes. A platinum wire was utilized as a counter electrode and a saturated calomel electrode (SCE) was employed as a reference electrode. In the experiments, indium tin oxide (ITO)/glass substrate surfaces with an area of about 1.32 cm^2 were employed as working electrodes. The cleaning process was done in an environment containing acetone for 5 min and then in an ethanol-containing environment for 5 min. Finally, the surfaces were rinsed with deionized water for 10 min using an ultrasonic bath. The cleaned ITO/glass substrates used in the experiments had a sheet resistance of approximately 8–12 Ω/sq. To obtain the ternary Ni–Co–Cu deposits with different compositions, three different bath solutions composed of fixed 0.070 M Ni sulfate, 0.1 M boric acid, and 0.0070 M Cu sulfate but various Co sulfate concentrations such as 0.025, 0.035, and 0.050 M were freshly made. The temperature and the pH values of the freshly made bath solutions were 25 $\pm$ 1 °C and 4.3 $\pm$ 0.1, respectively. In the experiments, the electrochemical fabrication of the ternary Ni–Co–Cu deposits was carried out at a fixed deposition cathode potential of –1.5 V versus SCE. Experimental processes were carried out at ambient temperature and pressure without stirring. Deposits with thicknesses of about 0.6 μm were fabricated by controlling the charge based on Faraday's law.

The structural features of the produced ternary Ni–Co–Cu deposits were characterized using a PANalytical Empyrean X-ray diffraction (XRD) technique. The XRD patterns were recorded from 40° to 55° with 0.025° steps using CuKα radiation with λ= 0.154059 nm. The surface morphological and compositional characterizations were carried out with a Zeiss Supra 40Vp scanning electron microscope (SEM) and an energy dispersive X-ray (EDX) spectroscope attached to a SEM.

3. Results and discussion

The aim of this study was to investigate the effect of the deposit composition on structural features and surface morphologies of Ni–Co–Cu/ITO deposits electrochemically fabricated from a sulfate-based bath solution with different Co ion concentrations at ambient temperature. The potentiostatic current–time transient curves recorded for the first 40 s to follow the growth period of the ternary Ni–Co–Cu deposits during the electroplating fabrication process are shown in Figure 1 with respect to the Co ion concentration. As seen from Figure 1, enhancement in the Co ion concentration leads to a very slight change in the current density. In addition to that, the current density occurring between the anode and the cathode is almost stable irrespective of the Co

ion concentration, showing that the Ni–Co–Cu deposits can be electroplated uniformly on the ITO substrates under these electroplating conditions.

The compositional analyses of the resultant deposits were carried out according to the Co ion concentration and the results obtained from the EDX analyses are shown in Figure 2 and listed in the Table. An increase in the Co ion concentration of the bath solution from 0.025 to 0.050 M enhances the Co content from 30.2 to 49.4 wt.% but diminishes the Ni and Cu contents from 50 to 38.9 wt.% and from 19.8 to 11.7 wt.%, respectively. The influence of Co ion concentration on the Co–Ni(Cu)/Cu multilayers, which were electrochemically deposited from citrate-based baths, was also investigated in a previous study [7]. It was found that the deposit composition is strongly affected by changing the Co ion concentration in the bath compared to the Ni ion concentration. That study also showed that the Co content in the deposit structure increases, but the Ni and Cu contents diminish as the Co ion concentration of the bath is enhanced [7]. Consequently, in this study, three different ternary deposits, i.e. Ni–30.2Co19.8Cu, Ni–39.2Co16.5Cu, and Ni–49.4Co11.7Cu, were obtained from sulfate-based bath solutions with various Co ion concentrations using the electrochemical deposition technique.

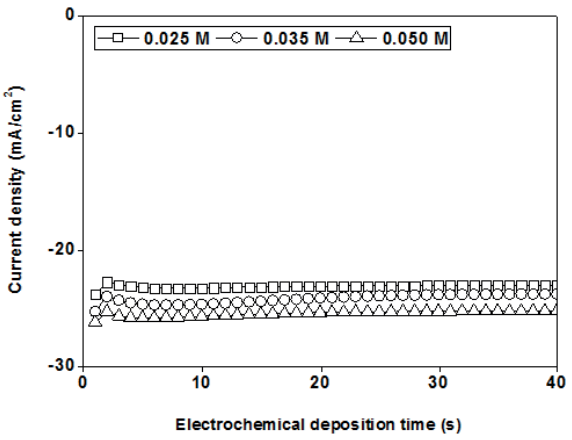

Figure 1. Potentiostatic current–time transient curves with respect to the Co ion concentration in the bath solution.

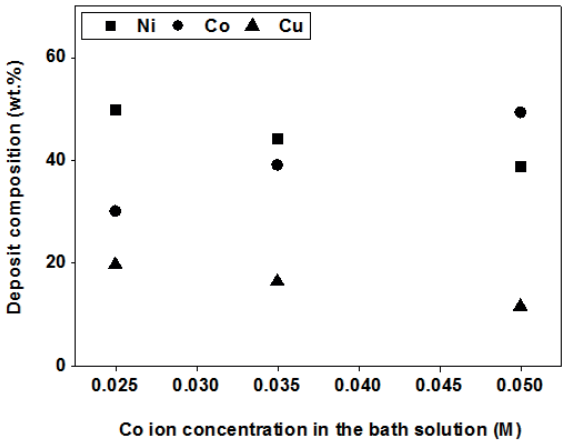

Figure 2. The compositional changes of the ternary Ni–Co–Cu deposits according to the Co ion concentration in the bath solution.

Table. Co/Ni ratio, crystallite size, interplanar spacing, and average diameter of the agglomerated clusters according to the deposit composition in electrochemically fabricated ternary Ni–Co–Cu deposits.

Deposit composition (wt.%)			Co/Ni ratio	Crystallite size (nm)	Interplanar spacing (nm)	Average diameter of the agglomerated clusters (nm)
Ni	Co	Cu				
50.0	30.2	19.8	0.604	18.5 ± 0.4	$0.20411 \pm 1.2 \times 10^{-5}$	1172 ± 283
44.3	39.2	16.5	0.892	17.9 ± 0.4	$0.20420 \pm 1.5 \times 10^{-5}$	1330 ± 298
38.9	49.4	11.7	1.270	16.8 ± 0.4	$0.20426 \pm 1.4 \times 10^{-5}$	1694 ± 197

An electrochemically fabricated deposit comprising Ni, Fe, and Co metals exhibited anomalous codeposition behavior under many different operating conditions [11] and the reason for that phenomenon was explained [12]. In this study, the formation of anomalous codeposition behavior was also studied since the Ni, Co, and

Cu contents in the deposit structure were determined to be different from those in the bath solution. The relation between the Co percentage in the deposit structures and the Co ion percentage in the bath solutions according to the Co ion concentration is demonstrated in Figure 3. The Co percentages in the deposit structures were always higher than the Co ion percentages in the bath solutions, suggesting that the less noble Co metal is preferentially electroplated. These results indicated that the electrochemical deposition characteristic of Ni–Co is an anomalous codeposition irrespective of the Co ion concentration. An anomalous codeposition was also reported in electrochemically fabricated ternary Ni–Co–Cu deposits grown from the sulfate [1, 13] and sulfate/citrate-based bath solutions [2–4,14]. In this work, the influence of the Co ion concentration on the degree of the anomalous codeposition behavior was also studied by means of the selective ratio. The value of the selective ratio of the Co–Ni was determined by using the relation described in a previous work [15]:

Selective ratio of the Co–Ni = (Co/Ni ratio within the deposit) / (Co/Ni ratio within the bath solution)

The same procedure was also applied to obtain the values of the selective ratio of both Ni–Cu and Co–Cu. The behavior of the selective ratios of the Co–Ni, Ni–Cu, and Co–Cu against the Co ion concentration of the bath solution is displayed in Figure 4. The value of the selective ratio of the Co–Ni increased slightly when the Co ion concentration increased, revealing that the influence of the Co ion concentration on the degree of the anomalous codeposition behavior is negligible. Also, according to Figure 4, Cu as a more noble metal is preferentially electroplated compared to less noble Ni and Co metals since the values of the selective ratios of both Ni–Cu and Co–Cu are always lower than 1. These results demonstrated the existence of the normal codeposition of both Ni–Cu and Co–Cu independently of the Co ion concentration in the bath. Besides, an enhancement in the Co ion concentration resulted in a slight increment in the values of the selective ratio of both Ni–Cu and Co–Cu, similar to the selective ratio of Co–Ni.

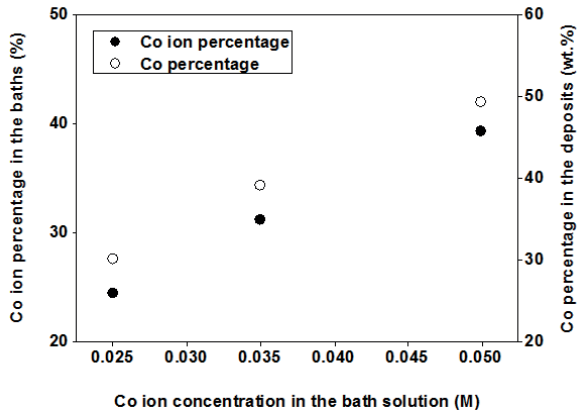

Figure 3. The relation between the Co percentage in the deposit structure and Co ion percentage in the bath solution according to the Co ion concentration.

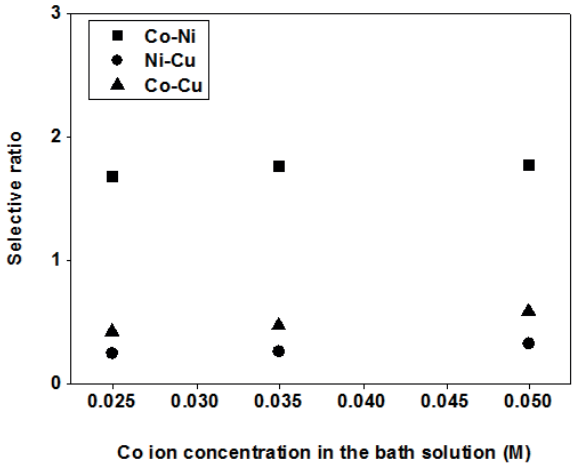

Figure 4. The behavior of the selective ratios of the Co–Ni, Ni–Cu, and Co–Cu against the Co ion concentration in the bath solution.

XRD measurements were performed for all deposits to investigate the structural properties in relation to the deposit composition. The recorded XRD patterns of the ternary Ni–30.2Co19.8Cu, Ni–39.2Co16.5Cu, and Ni–49.4Co11.7Cu deposits and an uncoated ITO/glass substrate are demonstrated in Figure 5. The crystalline structures were found to be fcc and no hexagonal close-packed (hcp) Co phase structure was detected for these

chemical compositions in any deposits. In previous studies, it was shown that binary Ni–Co deposits with similar Co contents exhibit the fcc (111) and (200) diffraction peaks without the diffraction peaks of the hcp Co phase structure [10,16]. Furthermore, the diffraction peaks of the hcp Co phase did not appear in the XRD patterns of the ternary Ni–Co–Cu deposits with similar [2,4] or much higher Co contents [1,13]. As seen in Figure 5, the deposits have two adjacent diffraction peaks in the fcc (111) and (200) phase structures. The diffraction peaks appeared at 2θ angles lower than 44° ($\sim 43.33^\circ$) and 51° ($\sim 50.44^\circ$) belong to the (111) and (200) diffraction peaks of the pure Cu phase, respectively. However, the (111) and (200) diffraction peaks of the Ni–Co phase appear at 2θ angles higher than 44° and 51°, respectively. The presence of these two adjacent diffraction peaks reflects the formation of a dual phase structure comprising Cu and Ni–Co phases in the growth process of the ternary Ni–Co–Cu/ITO deposits electrochemically fabricated from sulfate-based baths without additives. In earlier studies, binary Ni–Cu/ITO [17,18] and ternary Ni–Cu–Fe/ITO [6] deposits electrochemically fabricated from sulfate-based baths without additives exhibited a dual phase structure. The existence of a dual phase structure in ternary Cu–Co–Ni deposits consisting of pure Ni and Cu phases electrochemically grown from sulfate-based bath solutions without additives on polycrystalline titanium sheets was also reported [1,13]. However, it was shown that ternary Ni–Cu–Co deposits electrochemically fabricated from sulfate/citrate-based bath solutions with additives on the copper substrates [4] and without additives on the vitreous carbon substrates [2] exhibited a single phase structure. In addition to that, ternary Co–Ni–Cu deposits electrochemically grown from chloride bath solutions without additives on titanium foils were solid solutions [19]. As a result, when the findings of this study are evaluated together with those of previous studies, it may be suggested that the type of bath used in the experiments has a strong effect on the phase structure of electrochemically grown ternary Ni–Cu–Co deposits.

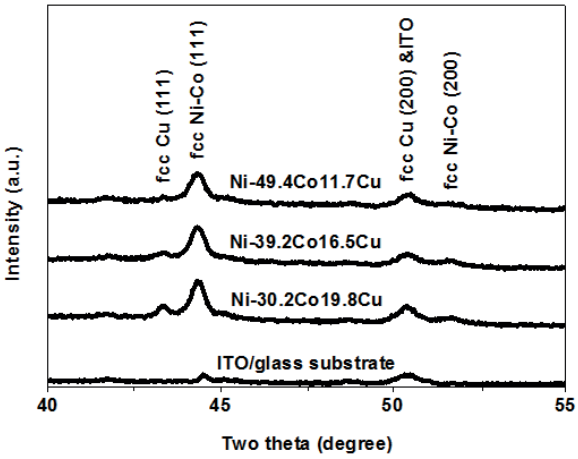

Figure 5. XRD patterns of the nanocrystalline ternary Ni–30.2Co19.8Cu, Ni–39.2Co16.5Cu, and Ni–49.4Co11.7Cu deposits and an uncoated ITO/glass substrate.

As seen from the XRD patterns in Figure 5, the preferred crystallographic orientation is in the (111) direction for all deposits since the deposits have crystallites with a significantly stronger (111) plane orientation than the (200) one regardless of the deposit composition. The same preferred crystallographic orientation was also revealed in electrochemically grown single Ni [20–24], binary Ni–Fe [8], Ni–Co [10], Ni–Cu [17,18,25], ternary Ni–Cu–Fe [6,26], and Cu–Co–Ni [13] metallic deposits. However, the intensity of the diffraction peaks shows

a strong dependence on the deposit composition. An increase in the Co content gives rise to a decrement in the intensities of both Ni–Co (111) and (200) diffraction peaks. In an earlier study [10], it was shown that the intensities of both Ni–Co (111) and (200) diffraction peaks decrease when the Co content in electrochemically fabricated binary Ni–Co deposits is enhanced. The intensity of the diffraction peaks related to the Cu phase structure strongly decreased with increasing Co content due to a simultaneous reduction of the Cu content in the deposit structure (Figure 5). Consequently, the XRD analyses showed that an increment in the Co content of the ternary Ni–Co–Cu deposits reduces the overall crystallinity. Lower degree of crystallinity at higher Co contents represents an increase in the number of defects acting as scattering centers [27].

On the other hand, there is a slight shift in the angular position of the Ni–Co (111) diffraction peak towards lower 2θ values with increasing Co content in the deposit structure. Therefore, the deposits have different interplanar spacing values. In order to estimate the full width at half maximum (FWHM) and the interplanar spacing values for the main (111) diffraction peak and to determine the relative integral intensity of the Ni–Co (111) diffraction peak with respect to the Cu (111) diffraction peak, the background-corrected XRD diffraction patterns were fit by Lorentzian curves. The enlarged versions of the measured data and fitting curves for the Ni–Co (111) and Cu (111) diffraction peaks of the deposits with different compositions are shown in Figure 6. The interplanar spacings for the main Ni–Co (111) diffraction peak were estimated by using Bragg's law from the XRD data [28]. The determined values of the interplanar spacing and Co/Ni ratios of the deposit structures are shown in Figure 7 according to the Co content in the deposit structure and are also summarized in the Table. As seen from the Table, the values of the interplanar spacing are between the values of the interplanar spacings of pure fcc $Co_{(111)}$ (0.20465 nm) [29,30] and pure fcc $Ni_{(111)}$ (0.2034 nm) [31] for all deposits. However, an increase in the Co content results in a slight increase in the interplanar spacing. These differences of interplanar spacing according to the Co content can be related to an increase in the Co/Ni ratio of the deposit structure (Figure 7). This is reasonable since the interplanar spacing of the fcc $Co_{(111)}$ is higher compared to the interplanar spacing of the fcc $Ni_{(111)}$. There is a shift in the position of the Ni–Co (200) diffraction peak towards lower 2θ values with increasing Co content in the deposit structure. This results in an increment in the interplanar spacing of the Ni–Co (200) diffraction peak. Furthermore, a change in the deposit composition leads to a change in the relative integral intensity of the Ni–Co (111) diffraction peak with respect to that of Cu (111). The percentage of the relative integral intensity of the Ni–Co (111) diffraction peak with respect to Cu (111) is described as $[I_{Ni-Co(111)} / I_{Ni-Co(111)} + I_{Cu(111)}] \times 100$ and the obtained values are shown in Figure 8 according to the Co content within the deposits. As seen in Figure 8, the values are about 84%, 88%, and 97% for the ternary Ni–30.2Co19.8Cu, Ni–39.2Co16.5Cu, and Ni–49.4Co11.7Cu deposits, respectively. Thus, an important result is revealed by this structural analysis: increasing the Co (Cu) content in the deposit structure enhances the relative integral intensity of the Ni–Co (111) (Cu (111)) diffraction peak with respect to Cu (111) (Ni–Co (111)), which indicates that the strength of the Ni–Co (111) (Cu (111)) phase increases with respect to the Cu (111) (Ni–Co (111)) phase when the Co (Cu) content in the ternary Ni–Co–Cu deposit increases.

The width of the Ni–Co (111) diffraction peak also changes when the Co content in the deposit structure is increased, reflecting that a change in the deposit composition affects the size of the crystallites. The crystallite size, D, depending on the deposit composition is estimated with the Scherrer formula [28]:

$$D = \frac{0.9\lambda}{Bcos\theta},$$

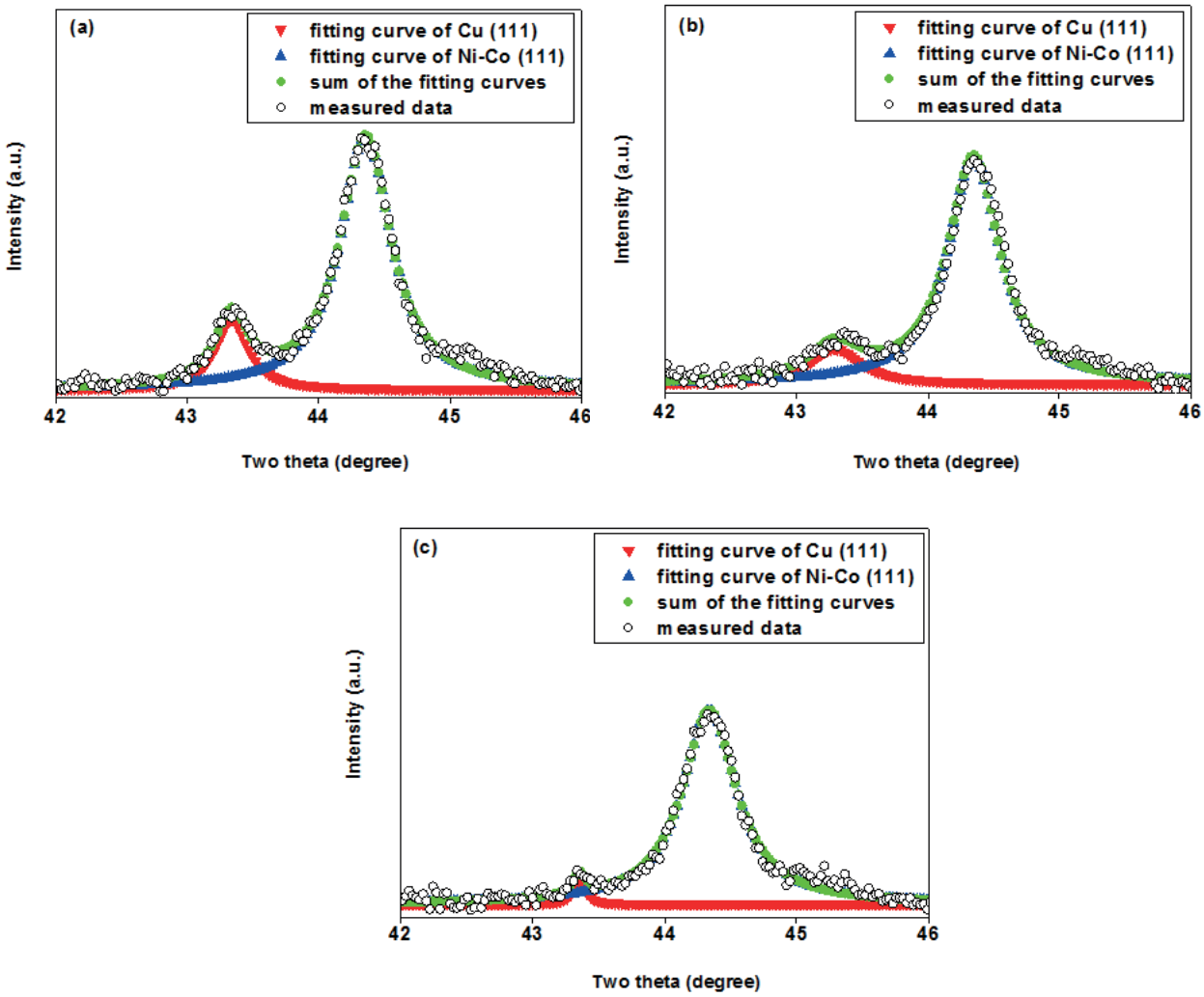

Figure 6. Enlarged versions of the measured data and fitting curves for the Ni–Co (111) and Cu (111) diffraction peaks of the nanocrystalline ternary deposits: a) Ni–30.2Co19.8Cu, b) Ni–39.2Co16.5Cu, and c) Ni–49.4Co11.7Cu.

where θ is the diffraction angle, λ is the wavelength of CuKα radiation, and B is the FWHM of the Ni–Co (111) diffraction peak. The determined values of crystallite size are listed in the Table with respect to the deposit composition. The findings suggest that all deposits fabricated in the experiments have nanostructured crystallites since their crystallite sizes were between 16.8 and 18.5 nm. Also, a decrease in the crystallite size from 18.5 to 16.8 nm is achieved when the Co content in the deposit structure increases from 30.2 to 49.4 wt.%, due to the refining effect of Co [4,24]. In a previous study [1], it was reported that the crystallite sizes of ternary Cu–Co–Ni deposits comprising 8–24 at.% Cu and 59–74 at.% Co were in the range of 35 to 64 nm. Although these deposits had much higher Co contents compared with those of the deposits produced in this study, their crystallite sizes were much larger. In another study [4], it was shown that the ternary Ni–6.3Cu23.8Co, Ni–34.7Cu15Co, and Ni–13.5Cu37.8Co deposits had crystallite sizes ranging between 21.2 and 22.7 nm, which are slightly larger than the crystallite sizes of the deposits grown in this study. It was also reported that ternary Ni–49.1Cu23.6Co and Ni–44Cu33.6Co deposits exhibited relatively smaller crystallite sizes of 10.5 and 10.3 nm, respectively [4].

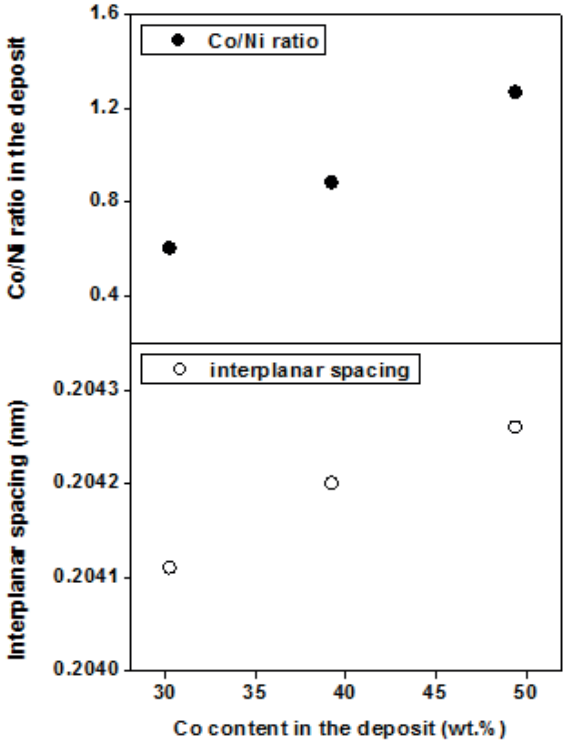

Figure 7. The interplanar spacing and Co/Ni ratios of the deposit structure as a function of the Co content.

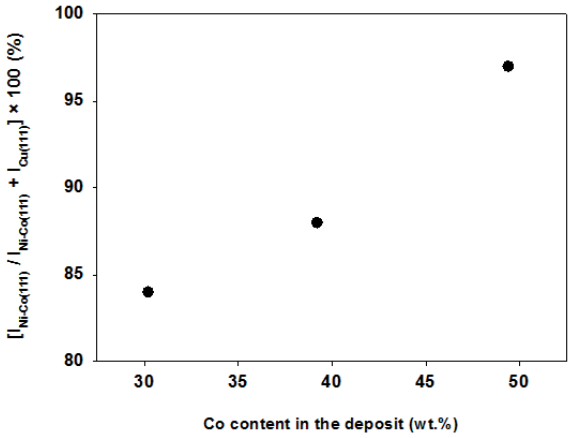

Figure 8. Percentages of the relative integral intensity of the Ni–Co (111) diffraction peak with respect to Cu (111) according to the Co content within the deposit.

Not only structural properties but also surface morphologies were considerably affected by changing the deposit composition. SEM micrographs of the ternary Ni–Co–Cu deposits with various compositions are shown in Figure 9. The surface structures of the deposits showed a dense and noncracked morphology and they were composed of bottom and upper parts. The bottom part of the surface structure consisted of much smaller round particles, while the upper part was composed of larger agglomerated clusters. The average diameter and the density of these larger agglomerated clusters show a strong dependence on the deposit composition. As seen from the SEM images, an increment in the Co content results in a significant decrement in the density of the larger agglomerated clusters. The deposits possess larger agglomerated clusters with different diameters varying roughly between 778 and 1889 nm. As summarized in the Table, the average diameters of those clusters are 1172, 1330, and 1694 nm for the ternary Ni–30.2Co19.8Cu, Ni–39.2Co16.5Cu, and Ni–49.4Co11.7Cu deposits, respectively. This reveals that the average diameter of the larger agglomerated clusters increases with increasing Co content in the deposit structure. An increment in the size of the agglomerated clusters indicates a rougher deposit surface with higher Co contents. The deposits grown in this study exhibit a quite different morphological structure compared to those revealed in previous studies [1,4,13,19]. Microsticks and speci?c growth orientation [1], agglomerated clusters and a great number of pores [4], and dendritic-like structures [13,19] on the deposit surfaces were detected. These differences in the morphological features can be attributed to not only compositional differences but also different operating conditions applied in the experiments such as substrate type, additives, bath concentration, bath type, deposition potential and/or current density, temperature, and pH value of the bath solution. It is well known that these operating differences significantly

affect the morphological properties of electrochemically fabricated materials. Further EDX analyses performed on different upper and bottom parts of the surface structure of the ternary Ni–30.2Co19.8Cu deposit indicated that the agglomerated clusters that appeared on the upper part contained more Cu content and less Ni and Co contents (40.2 wt.% Ni, 27.8 wt.% Co, and 32 wt.% Cu) than the bottom part (56.4 wt.% Ni, 32 wt.% Co, and 11.6 wt.% Cu). Similar findings were also revealed in electrochemically fabricated Ni–Cu [17], Ni–Cu–Fe [6], and Cu–Co–Ni [1,13] deposits exhibiting a dual phase structure. As a result, the ternary Ni–Co–Cu deposits electrochemically fabricated on ITO/glass substrates in this study exhibited quite different structural and morphological features, not only according to their chemical compositions but also compared to those of the deposits grown on different substrates in previous studies [1,2,4,13,19].

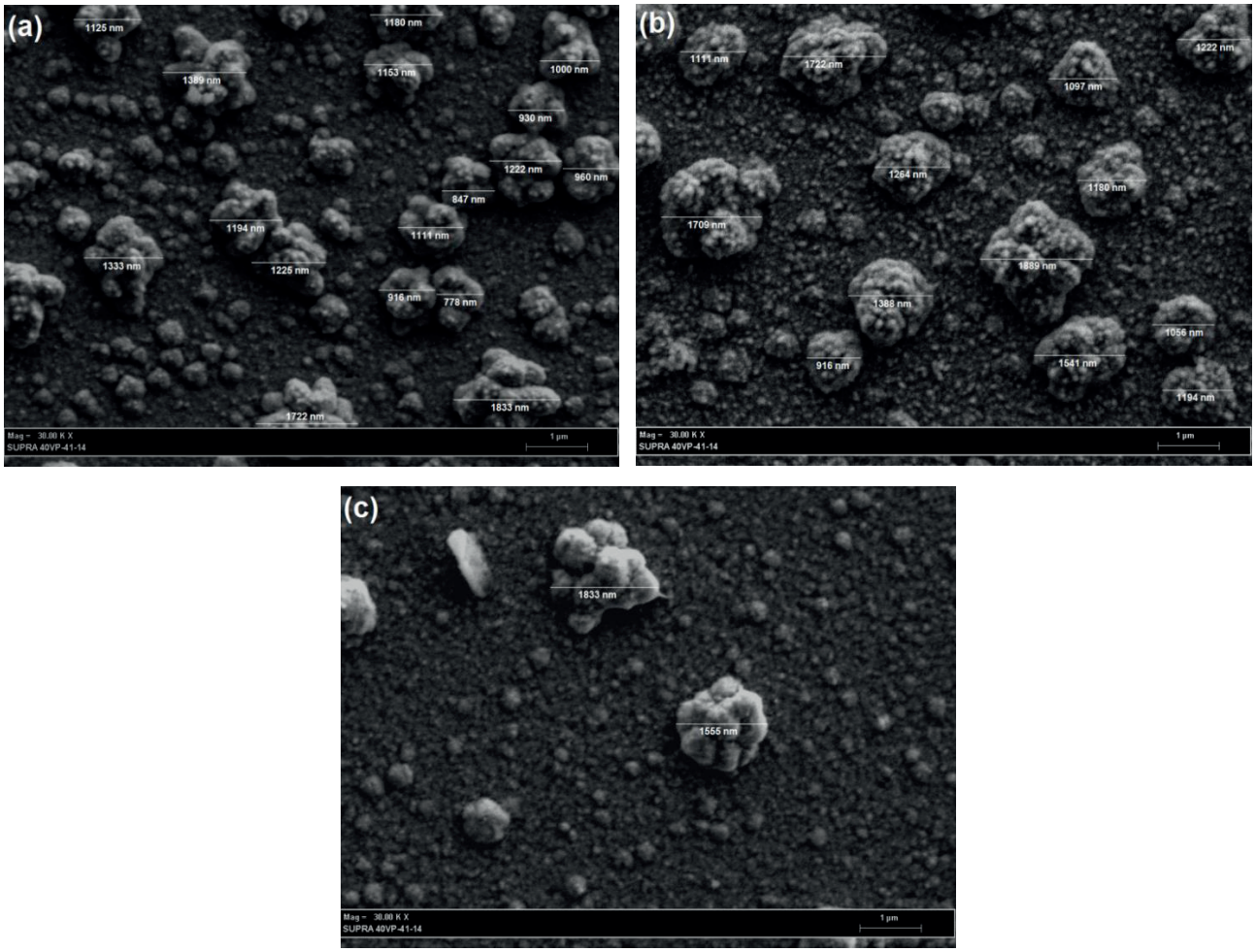

Figure 9. SEM images of the electrochemically fabricated nanocrystalline ternary deposits: a) Ni–30.2Co19.8Cu, b) Ni–39.2Co16.5Cu, and c) Ni–49.4Co11.7Cu.

4. Conclusions

In this study, three different ternary deposits, Ni–30.2Co19.8Cu, Ni–39.2Co16.5Cu, and Ni–49.4Co11.7Cu, were electrochemically achieved from sulfate-based bath solutions including various Co ion concentrations without additives at ambient temperature. Increasing the Co ion concentration enhanced the Co content

but reduced the Ni and Cu contents. The Ni–Co was codeposited anomalously while the electrochemical deposition characteristics of Ni–Cu and Co–Cu revealed normal codeposition. The amount of Co ions in the bath solution had an insignificant effect on the degree of the anomalous codeposition behavior. All deposits with (111) preferred crystallographic orientation exhibited segregated fcc Cu and Ni–Co diffraction peaks. An enhancement in the Co content from 30.2 to 49.4 wt.% reduced the overall crystallinity and provided a decrement in the crystallite size from 18.5 to 16.8 nm. The strength of the Ni–Co (111) (Cu (111)) phase with respect to the Cu (111) (Ni–Co (111)) phase increased when the Co (Cu) content in the deposit structure increased. Also, according to the results obtained from the structural analysis, an increment in the Co/Ni ratio of the deposit structure resulted in an increment in the interplanar spacing of the Ni–Co (111) diffraction peak. An increase in the average diameter from 1172 to 1694 nm but a strong decrement in the density of the larger agglomerated clusters occurred when the Co content in the deposit structure was enhanced from 30.2 to 49.4 wt.%. Consequently, a change in the deposit composition caused not only quite different structural properties but also quite different morphological features in electrochemically grown ternary Ni–Co–Cu/ITO deposits.

Acknowledgment

This work was financially supported by the Scientific Research Projects Commission of Bartın University under project number 2013.2.98.

References

[1] Karpuz, A.; Kockar, H.; Alper, M. *J. Mater. Sci. Mater. Electron.* **2014**, *25*, 4483-4488.

[2] Gómez, E.; Pané, S.; Vallés, E. *Electrochim. Acta* **2005**, *51*, 146-153.

[3] Karahan, I. H.; Bakkaloglu, O. F.; Bedir, M. *Pramana J. Phys.* **2007**, *68*, 83-90.

[4] Chai, Z.; Jiang, C.; Zhao, Y.; Wang, C.; Zhu, K.; Cai, F. *Surf. Coat. Technol.* **2016**, *307*, 817-824.

[5] Sarac, U.; Baykul, M. C. *Adv. Mater. Sci. Eng.* **2013**, 2013, 1-7.

[6] Sarac, U.; Baykul, M. C. *J. Mater. Sci. Mater. Electron.* **2014**, *25*, 2554-2560.

[7] Dulal, S. M. S. I.; Charles, E. A. *J. Alloys Compd.* **2008**, *455*, 274-279.

[8] Saraç, U.; Kaya, M.; Baykul, M. C. *Turk. J. Phys.* **2017**, *41*, 536-544.

[9] Saraç, U.; Kaya, M.; Baykul, M. C. *Turk. J. Phys.* **2018**, *42*, 136-145.

[10] Sarac, U.; Baykul, M. C.; Uguz, Y. *J. Supercond. Nov. Magn.* **2015**, *28*, 3105-3110.

[11] Brenner, A. *Electrodeposition of Alloys Principles and Practice*; Academic Press: New York, NY, USA, 1963.

[12] Yang, Y. *Int. J. Electrochem. Sci.* **2015**, *10*, 5164-5175.

[13] Karpuz, A.; Kockar, H.; Alper, M. *IEEE T. Magn.* **2014**, *50*, 1-4.

[14] Pané, S.; Gómez, E.; Vallés, E. *J. Electroanal. Chem.* **2006**, *596*, 87-94.

[15] Phan, N. H.; Schwartz, M.; Nobe, K. *J. Appl. Electrochem.* **1991**, *21*, 672-677.

[16] Sarac, U.; Baykul, M. C.; Uguz Y. *J. Supercond. Nov. Magn.* **2015**, *28*, 1041-1045.

[17] Sarac, U.; Baykul, M. C. *J Alloy Compd.* **2013**, *552*, 195-201.

[18] Sarac, U.; Öksüzoğlu, R. M.; Baykul, M. C. *J. Mater. Sci. Mater. Electron.* **2012**, *23*, 2110-2116.

[19] Wang, C.; Li, W.; Lu, X.; Xie, S.; Xiao, F.; Liu, P.; Tong, Y. *Int. J. Hydrogen Energy* **2012**, *37*, 18688-18693.

[20] Nzoghe-Mendome, L.; Ebothé, J.; Aloufy, A.; Kityk, I. V. *J. Alloys Compd.* **2008**, *459*, 232-238.

[21] Nzoghe-Mendome, L.; Aloufy, A.; Ebothé, J.; Hui, D.; El Messiry, M. *Mater. Chem. Phys.* **2009**, *115*, 551-556.

[22] Nzoghe-Mendome, L.; Aloufy, A.; Ebothé, J.; El Messiry, M.; Hui, D. *J. Cryst. Growth* **2009**, *311*, 1206-1211.

[23] Saitou, M.; Makabe, A.; Tomoyose, T. *Surf. Sci.* **2000**, *459*, L462-L466.

[24] Chu, S. Z.; Wada, K.; Inoue, S.; Todoroki, S. *Electrochim. Acta* **2003**, *48*, 3147-3153.

[25] Sarac, U.; Baykul, M. C. *J. Mater. Sci. Mater. Electron.* **2013**, *24*, 2777-2784.

[26] Sarac, U.; Kaya, M.; Baykul, M. C. *J. Phys. Conf. Ser.* **2016**, 766, 1-6.

[27] Tuna, O.; Selamet, Y.; Aygun, G.; Ozyuzer, L. *J. Phys. D Appl. Phys.* **2010**, *43*, 1-7.

[28] Cullity, B. D. *Elements of X-Ray Diffraction, 2nd Edition*; Addison-Wesley Publishing Company: Reading, MA, USA, 1978.

[29] Rafaja, D.; Schimpf, C.; Schucknecht, T.; Klemm, V.; Péter, L.; Bakonyi, I. *Acta Mater.* **2011**, *59*, 2992-3001.

[30] Rafaja, D.; Schimpf, C.; Klemm, V.; Schreiber, G.; Bakonyi, I.; Péter, L. *Acta Mater.* **2009**, *57*, 3211-3222.

[31] Kolonits, T.; Jenei, P.; Tóth, B. G.; Czigány, Z.; Gubicza, J.; Péter, L.; Bakonyi, I. *J. Electrochem. Soc.* **2016**, *163*, D107-D114.